Published in final edited form as:
Drug Metab Dispos. 2008 October ; 36(10): . doi:10.1124/dmd.108.020354.

PHARMACOKINETICS OF THE NOVEL NICOTINIC RECEPTOR ANTAGONIST, *N,N'*-DODECANE-1,12-DIYL- *bis*-3-PICOLINIUM DIBROMIDE (bPiDDB) IN THE RAT

Zaineb A. Fadhel Albayati, **Linda P. Dwoskin**, and **Peter A. Crooks**
Department of Pharmaceutical Sciences College of Pharmacy, University of Kentucky, Lexington KY 40536

Abstract

Plasma and brain concentrations of the nicotinic acetylcholine receptor (nAChR) antagonist and blood-brain barrier choline transporter substrate, *N,N'*-dodecane-1,12-diyl-*bis*-3-picolinium dibromide (bPiDDB), were analyzed by liquid β-scintillation spectrometry following administration of [$^{14}CH_3$]-bPiDDB to male Sprague-Dawley rats. Plasma concentrations of [$^{14}CH_3$]-bPiDDB were determined at 10 time points over 3 hr. Absolute plasma bioavailabilities (1, 3 and 5.6 mg/kg, s.c.) were 80.3%, 68.2% and 103.7%, respectively. bPiDDB (1, 3 and 5.6 mg/kg) afforded C_{max} values of 0.13, 0.33 and 0.43 μg/mL, respectively, T_{max} values of 5.0, 6.7 and 8.8 min, respectively, and $t_{1/2}$ values of 11.2, 19.5 and 16.9 min, respectively. Mean $AUC^{0-\infty}$ (μg.min/mL) and mean C_{max} (μg/mL) values were dose-dependent (r^2=0.9361 and 0.7968, respectively) over the dose range studied. No metabolism of [$^{14}CH_3$]-bPiDDB was detected with any dose of bPiDDB administered. Only moderate protein binding (63–65% in plasma, 59–62% in brain supernatant) was observed, which was reversible. Brain concentrations, and brain/plasma ratios of bPiDDB after a single 5.6 mg/kg s.c. dose over 5–60 min ranged from 0.09–0.33 μg/g brain tissue and were maximal at 10 min post-injection, representing about 0.6 % of the administered dose. Brain/blood ratio (0.18 at 5 min to 0.51 at 60 min post injection) was observed, indicating that clearance from brain is slower than clearance from plasma. The results show that bPiDDB is distributed rapidly from the site of injection into plasma, affords good plasma concentrations, and appears to reach brain tissues via facilitated transport by the blood-brain barrier choline transporter to afford therapeutically relevant concentrations in rat brain.

Habitual tobacco use is a major contributing factor to many preventable health problems, including lung cancer, emphysema and cardiovascular disease. The Center for Disease Control and Prevention describes tobacco use as the single most important preventable risk to human health and an important cause of premature death worldwide (Chen and Mannino, 1999; Mannino and Braman, 2007). Nicotine replacement therapies (e.g., nicotine gum, transdermal patch, nasal spray, and inhaler) have been used to relieve craving and withdrawal symptoms and result in diminished exposure of the smoker to toxic components of tobacco smoke. Several non-nicotine therapies have been used as treatments for nicotine addiction, including bupropion, an antidepressant medication with neuronal nicotinic receptor (nAChR) antagonist properties (Dwoskin et al, 2006) and varenicline, a partial agonist at α4β2 nAChRs and full agonist at α7 nAChRs (Coe et al., 2005; Mihalak et al., 2006). Mecamylamine, a nonselective antagonist at both central and peripheral nAChRs, has

Address correspondence to: Peter A. Crooks, Ph.D, George A. Digenis Professor in Drug Design and Discovery, Department of Pharmaceutical Sciences, College of Pharmacy, Lexington, KY 40536-0082. Tel: (859) 257-1718; Fax: (859) 257-7585; Email: pcrooks@email.uky.edu.

been developed for use as a tobacco cessation agent, but its clinical use has been precluded by peripheral side effects, such as dry mouth and constipation (Lundahl et al., 2000). Despite some success of the currently available pharmacotherapies, relapse rates continue to be high, indicating that novel medications are still needed.

Our research group has recently synthesized a library of *bis*-azaaromatic quaternary ammonium analogs that act as central nAChR antagonists (Ayers et al., 2002). bPiDDB (*N*,*N*'-dodecane-1,12-diyl-*bis*-3-picolinium dibromide, Figure 1), is a novel polar *bis*-quaternary ammonium salt currently being developed as a nAChR antagonist that inhibits nAChRs mediating nicotine-evoked dopamine release. bPiDDB potently inhibits nicotine-evoked dopamine release from superfused rat striatal slices with an IC_{50} value of 5 nM. In addition, bPiDDB selectively decreases the reinforcing effect of nicotine (Dwoskin et al. 2004; Neugebauer et al., 2006). Recently, in vivo microdialysis studies have demonstrated that bPiDDB dose-dependently reduces nicotine-evoked extracellular dopamine release in rat nucleus accumbens (Rahman, et al., 2007). Since bPiDDB is a polar, cationic molecule, it might be expected not to penetrate the blood-brain barrier and bind to central nAChRs. However, recent studies have shown that bPiDDB is an excellent substrate for the blood-brain barrier choline transporter (Geldenhuys et al., 2005; Lockman et al., 2007) and accesses brain via facilitated transport.

The objective of the current investigation was to determine the plasma pharmacokinetic parameters, blood-brain barrier permeation, and protein binding of [$^{14}CH_3$]-bPiDDB in rats following s.c. administration, as a first step towards understanding the overall pharmacokinetic profile of this novel nAChR antagonist. The s.c. route was chosen in the current pharmacokinetic studies, since this route of administration was used in the behavioral studies, which will enable behaviorally relevant brain concentrations of bPiDDB to be determined.

Materials and Methods

Chemicals

bPiDDB (*N*,*N*'-dodecane-1,12-diyl-*bis*-3-picolinium dibromide) was prepared using the method of Ayers et al. (2002). [$^{14}CH_3$]-bPiDDB (specific activity: 50 mCi/mmol) was obtained from Moravek Biochemicals (Brea, CA) and synthesized via 3-methylation of 4-chloropyridine with LDA and $^{14}CH_3I$, followed by hydrogenolysis with Pd/C-KOAc as catalyst to remove the 4-chloro group. Reaction of the resulting [$^{14}CH_3$]-3-picoline with 1, 12-dibromododecane afforded [$^{14}CH_3$]-bPiDDB; radiochemical purity was > 98% (Ayers et al., 2002). The chemicals employed in this study were of HPLC grade or equivalent quality. Acetonitrile, formic acid, ammonium formate, potassium chloride, and Bio-Safe NA scintillation cocktail were obtained from Fisher Scientific, Pittsburgh, PA. Heparin sodium injection, 10,000 USP units/mL, was purchased from Baxter Healthcare Corporation, Deerfield, IL. Nembutal sodium (pentobarbital sodium injection, USP) was obtained from Abbott Laboratories (North Chicago, IL).

Animals

All procedures involving animals were performed in compliance with the Institutional Animal Care and Use Committee (IACUC) of the University of Kentucky guidelines established by the 1996 NIH Guide for the Care and Use of Laboratory Animals. Male Sprague-Dawley rats (200–250 g) were obtained from Harlan Laboratories (Indianapolis, IN, USA) and housed two per cage with ad libitum access to food and water in the Division of Laboratory Animal Resources at the University of Kentucky, College of Pharmacy. Body weights at the time of dosing were 290–310 g. Rats were anesthetized with pentobarbital (40

mg/kg, i.p.) and surgically implanted with jugular and femoral vein cannulae for i.v. drug dosing and blood sampling, respectively. bPiDDB was injected s.c. in the back of the animal between the shoulders blades. For the first 3–4 days after surgery, the rats were observed for signs of infection at the surgical sites, yellowing of hair and hair texture, presence of blood around the eyes or nose, indications of loss of appetite, and decreased or absent fecal activity before the start of s.c. or i.v. dosing. The i.v. and s.c. dosing was performed in a parallel design.

Plasma Pharmacokinetics

Solutions of bPiDDB containing a tracer amount (50 μCi) of [$^{14}CH_3$]-bPiDDB were prepared in fresh phosphate buffered saline and filtered through a 0.2 μm filter. Groups of rats (n=3–5) were then injected with either 1, 3 or 5.6 mg/kg s.c. or 1 mg/kg, i.v. [$^{14}CH_3$]-bPiDDB via the jugular vein. Doses and route of administration were chosen based upon recent studies evaluating the effect of bPiDDB on behavioral activity in nicotine-dependent rats (Neugebauer et al., 2006). Blood samples (0.15 mL) were obtained at 0, 1, 5, 10, 15, 20, 30, 45, 60, 120, 180 min after injection of each dose. The withdrawn blood was replaced with heparinized saline (0.15 mL). Blood samples were centrifuged at 1200 g for 15 min and the plasma was separated. Plasma samples (50 μL) were mixed with 3.5 mL scintillation cocktail (Bio-Safe NA, Fisher Scientific, Pittsburgh, PA) and analyzed directly for the presence of [$^{14}CH_3$]-bPiDDB by β-scintillation spectrometric analysis (Tri-Carb 2200 TR Liquid Scintillation Spectrometer, PerkinElmer Life and Analytical Sciences, Shelton, CT).

Pharmacokinetic Analysis

The plasma pharmacokinetic parameters for bPiDDB in the rat were determined after both s.c. and i.v. administration. Data were analyzed utilizing a standard non-compartmental model using the program WinNonlin Professional (version 4.1, Pharsight Corporation, Mountain view, CA, USA). Both C_{max} and T_{max} were determined. The $AUC^{0\text{-}t}$ for the plasma concentration-time profile was determined using the linear-trapezoidal method (Whittaker and Robinson, 1967). $AUC^{0\text{-}\infty}$ was calculated as $AUC^{0\text{-}t} + C_t/k$, where C_t is the last measurable concentration of drug. The terminal half-life ($t_{1/2}$) of bPiDDB was calculated by dividing 0.693 by the terminal rate constant (k) obtained from the fitted concentration-time data. The area under the first moment curve (AUMC) for bPiDDB was determined using the linear-trapezoidal method with extrapolation to infinite time ($C_{last}*t_{last}/k + C_{last}/k^2$). Systemic clearance (CL) after the i.v. dose of bPiDDB was determined from Eq. 1:

$$\mathrm{CL}=\mathrm{Dose}/\mathrm{AUC}^{0-\infty} \quad \text{Eq.1}$$

volume of distribution at steady state (V_{ss}) for the i.v. dose of bPiDDB was determined from Eq. 2:

$$V_{ss}=\mathrm{Dose} \times \mathrm{AUMC}/(\mathrm{AUC})^2 \quad \text{Eq.2}$$

systemic bioavailability after s.c. administration of bPiDDB (*F*) was determined from Eq. 3:

$$F=[(\mathrm{Dose}_{\mathrm{i.v.}} \times \mathrm{AUC}_{\mathrm{s.c.}})/(\mathrm{Dose}_{\mathrm{s.c.}} \times \mathrm{AUC}_{\mathrm{i.v.}})] \times 100 \quad \text{Eq. 3}$$

where $AUC_{s.c.}$, $AUC_{i.v.}$, $Dose_{s.c.}$, and $Dose_{i.v.}$ represent the $AUC^{0\text{-}\infty}$ and corresponding dose for the s.c. and i.v. injections, respectively.

Brain Uptake Studies

Studies were carried out to determine the amount of bPiDDB in brain after a s.c. dose of 5.6 mg/kg. A solution (0.25 mL) of bPiDDB containing a tracer amount (50 μCi) of [$^{14}CH_3$]-bPiDDB and a total dose of 5.6 mg/kg bPiDDB was prepared in fresh phosphate buffered saline and filtered through a 0.2 μm filter. This dose was chosen since it has been shown to produce a robust behavioral effect in a rat model of nicotine-dependence (Bardo, unpublished studies). Non-catheterized male Sprague-Dawley rats (250–270g) were assigned randomly to one of six time points (n = 4 per group). Individual rats were euthanized at 0, 1, 5, 10, 15, 20 and 60 minutes after s.c. administration of bPiDDB. The brain was quickly removed, cleaned of surrounding tissue and veins, washed, weighed and homogenized (3 volumes 1.15% KCl/g brain tissue) for 2 min in a tissue homogenizer (Bio-Homogenizer M133/1281-0, Biospec Products, Inc., Barlesville, OK). Brain homogenate (4 mL) was mixed with an equal volume of a solution consisting of a 40:60 mixture of acetonitrile:formic acid 0.1%, pH, 2.3. The resulting mixture was then mixed with an equal volume of acetonitrile and centrifuged at 1200 g and 37 °C for 5 min. The supernatant was separated and evaporated to dryness under a stream of nitrogen. The residue was reconstituted in 0.2 mL of HPLC mobile phase consisting of 40:60 acetonitrile:2 mM ammonium formate, pH 2.3. Following decapitation, blood from the trunk of each rat at the time of euthanasia was also collected, and centrifuged at 1200 g and 37 °C for 5 min to obtain matching brain/plasma samples. The plasma samples (1 mL) were extracted with 6 volumes of acetonitrile and centrifuged at 1200 g for 15 min at 37 °C. The supernatant was separated and evaporated to dryness under a stream of nitrogen, and the resulting residue was dissolved in 0.2 mL of 40:60 acetonitrile/2 mM ammonium formate, pH 2.3. To determine [^{14}C]-bPiDDB and its metabolites, plasma and brain homogenate samples containing [^{14}C]-bPiDDB were each mixed with an authentic sample of bPiDDB to produce a final concentration of 0.01 mg/mL, which acted as a UV-absorbing standard, and an aliquot of each final mixture (20 μL) was injected onto a C_{18} Alltima column (5 μm, 150 × 3.2 mm; Alltech, Deerfield, IL, USA). The mobile phase consisted of 2 mM ammonium formate/acetonitrile 60:40, adjusted to pH 2.3 with 0.1% formic acid and containing 0.1% heptafluorobutyric acid; the flow rate was 0.4 mL/min. An Agilent 1100 series HPLC analytical system interphased to an L-4000 UV detector, an L-6000 intelligent pump, an AS-2000 autosampler, and a D-2500 chromato-integrator, Hitachi (Tokyo, Japan) was utilized. Fractions (∼ 70 μL/10 sec) eluting from the HPLC column were collected over 60 min for determination of ^{14}C-radiolabel in the column effluent. A volume of 20 μL identical to that injected onto the HPLC column was added to 3.0 mL of scintillation cocktail and analyzed directly by β-scintillation spectrometry to determine recovery of ^{14}C-radiolabel from the HPLC column. UV detection of a bPiDDB standard in plasma and brain homogenate samples was monitored continuously at 260 nm to determine the time of appearance of [$^{14}CH_3$]-bPiDDB in the column effluent.

Plasma Protein and Brain Protein Binding of bPiDDB in the Rat

The ability of bPiDDB to bind to plasma and brain proteins was determined using a modification of the ultrafiltration method of Cheng et al. (2004). A Centrifree Micropartition device (Amicon, Millipore Corporation, Beverly, MA, USA) was used for separating unbound bPiDDB from bound bPiDDB. bPiDDB was dissolved in water and added to either rat plasma (1 mL) or whole brain supernatant (1 mL) to afford concentrations of 0.04 and 0.1 mg/mL. The spiked plasma or brain supernatant was incubated for 15 min at 37 °C and an aliquot part (50 μL) analyzed by HPLC to determine bPiDDB concentration, as previously described. The ultrafiltrate was obtained by centrifugation at 1000 g and 37 °C for 10 min. The concentration of unbound bPiDDB in the filtrate was determined by HPLC analysis and UV detection at 260 nm, as previously described. Chromatography was performed on a C_{18} Alltima column (3.2 × 150 mm, 5 μm; Alltech, Deerfield, IL, USA). The

mobile phase consisted of 2 mM ammonium formate/acetonitrile 60:40, adjusted to pH 2.3 with 0.1% formic acid containing 0.1% heptafluorobutyric acid; the flow rate was 0.4 mL/min. A calibration curve was constructed from bPiDDB peak area versus concentration (r^2= 0.998) and was used to quantitate the amount of bPiDDB in the ultrafilitrate. The HPLC method was validated over the concentration range 1–200 μg/mL. The limit of quantitation (LOQ) was established at 1 μg/mL. The percent of free fraction of bPiDDB was calculated from Eq. 4.

$$\frac{\text{Concentration of bPiDDB in ultrafiltrate}}{\text{Concentration of bPiDDB in original spiked sample}} \times 100 \quad \text{Eq. 4}$$

In separate experiments to determine whether the observed binding of bPiDDB to plasma and brain protein was reversible or irreversible, radiolabeled [$^{14}CH_3$]-bPiDDB was utilized as a tracer compound. Plasma or brain supernatants containing [$^{14}CH_3$]-bPiDDB (concentrations of 1, 1.5, 15, 50, 100, 200, 250, and 400 μg/mL in both cases) were utilized. After incubation for 15 min at 37 °C, aliquot parts (50 μL) were taken, and radioactivity was determined by liquid scintillation spectrometry. The spiked plasma or brain sample was added to the sample reservoir of a Centrifree Micropartition device (Amicon, Millipore Corporation, Beverly, MA, USA) to separate unbound bPiDDB from bound bPiDDB. Samples were centrifuged for 10 min at 1000 g and 37 °C and radioactivity in the ultrafiltrate was determined by liquid scintillation spectrometry (Musick et al., 2007). The concentration of bound bPiDDB versus unbound bPiDDB was then plotted to afford the binding curve.

Statistics

Results were first analyzed by a one-way analysis of variance (ANOVA). Individual differences between means were determined using Tukey's *post hoc* test. $P < 0.05$ was considered statistically significant. Data are expressed as mean ± SEM.

Results

Figure 2 illustrates a typical high pressure liquid radiochromatogram of plasma from [$^{14}CH_3$]-bPiDDB -treated rats after a 5.6 mg/kg s.c. dose. An authentic UV-absorbing standard of bPiDDB was introduced into the plasma sample. UV detection of the co-injected standard was carried out at 260 nm while ^{14}C-radioactivity in the sample was monitored by β-scintillation spectrometry. The UV-absorbing bPiDDB standard eluted at 5.6 min and the ^{14}C-radioactivity in the sample was observed as a single peak that coeluted with the UV-absorbing bPiDDB standard. No other radiolabeled peaks were observed in the chromatogram. Analysis of ^{14}C-radioactivity in plasma samples obtained at 5 min, 10 min, 30 min, 60 min, 120 min, and 180 min post injection in rats that had received a dose of 5.6 mg/kg of [$^{14}CH_3$]-bPiDDB are shown in Figure 3. In all cases, individual chromatograms showed the presence of only one radiolabeled peak which coeluted with the UV-absorbing standard of bPiDDB. Recovery of plasma ^{14}C-radiolabel in the column effluent for the 5.6 mg/kg s.c. dose was 98.3% ± 0.8 at 5 min, 98.6% ± 1.0 at 10 min, 98.9% ± 0.6 at 30 min, 99.1% ± 0.5 at 60 min, 99.8% ± 0.8 at 120 min, and 99.3% ± 0.3 at 180 min. For bPiDDB, doses of 1 mg/kg s.c. and 3 mg/kg s.c. the recovery of plasma ^{14}C-radiolabel in the HPLC column effluents ranged from 98.2% to 99.4%, and 98.3% to 99.5%, respectively, over a 180 min time course.

Pharmacokinetic Analysis

Figure 4 illustrates the mean (± SEM) plasma concentration-time profiles for bPiDDB following the i.v. dose and the three s.c. doses of bPiDDB. bPiDDB was rapidly absorbed and distributed to the vascular compartment within 1 min of administration, and was detectable in plasma samples over a 1 min to 180 min time period. Table 1 provides a summary of the mean (± SEM) values for the pharmacokinetic parameters for bPiDDB after s.c. administration. The absolute systemic bioavailabilities (F) of bPiDDB (1, 3 and 5.6 mg/kg, s.c.) were obtained from Eq. 4 by comparing the mean AUC after i.v. and s.c. injections, and were 80.3%, 68.2% and 103.7%, respectively. bPiDDB (1, 3 and 5.6 mg/kg) afforded C_{max} values of 0.13, 0.33 and 0.43 μg/mL, respectively, T_{max} values of 5.0, 6.7 and 8.8 min, respectively, and $t_{1/2}$ values of 11.2, 19.5 and 16.9 min, respectively. The plasma concentration time curve ($AUC^{0-\infty}$) was selected as a pharmacokinetic index of drug exposure and reflects the total amount of drug absorbed by the body, irrespective of the rate of absorption. Mean $AUC^{0-\infty}$ (μg∗min/mL) and mean C_{max} (μg/mL) values for bPiDDB were dose dependent (r^2=0.9361 and 0.7968, respectively) over the 1–5.6 mg/kg dose range studied. Volume of distribution (V_{ss}) at steady state was 10.2 L (30 L/kg) and clearance (CL) was 0.6–0.9 L/h/kg over the dose range studied.

Brain Uptake Studies

In the brain uptake studies, HPLC analysis of both brain homogenates and matched plasma samples after s.c. injection of 5.6 mg/kg [$^{14}CH_3$]-bPiDDB afforded only one ^{14}C-radiolabeled peak in the HPLC radiochromatogram, which was identified as bPiDDB from its co-elution with a UV-absorbing authentic standard. As was observed in the plasma pharmacokinetic studies, percent recoveries of radiolabel from the chromatographic column eluents for both brain and matched plasma samples over a 60 min time course were close to 100% (Table 2). The plasma levels, brain levels, and brain/plasma ratios for the 5.6 mg/kg dose of bPiDDB over a 60 min time course, are provided in Table 2. Although bPiDDB could be detected in plasma as early as 1 min post injection, no significant concentrations of bPiDDB were detected in brain at this time point. bPiDDB brain concentrations were in the range 0.09–0.33 μg/g brain tissue over the 60 min time course and were maximal at 10 min. Brain/blood ratios of 0.18 at 5 min to 0.51 at 60 min post injection were observed.

Protein Binding

In the protein binding studies, 63–64% and 59–62% of bPiDDB was reversibly bound to rat plasma protein and brain protein, respectively, over the concentration range 0.04 to 0.10 mg/mL (Fig. 5). Protein binding isotherms constructed over a wide range of bPiDDB concentrations (1–400 μg/mL) for both plasma and brain homogenate indicated that the observed protein binding was reversible in nature.

Discussion

HPLC and radiometric analyses of plasma samples after s.c. administration indicated the absence of metabolites (60 min elution from the column) in plasma 5–180 min after [$^{14}CH_3$]-bPiDDB (5.6 mg/kg, s.c., Fig 3), which is consistent with the high recovery of ^{14}C-radiolabel in the column effluent. Thus, bPiDDB, behaves similarly to hexamethonium, a structurally related *bis*-quaternary ammonium drug, which is also poorly metabolized in rodents (Levine, 1959).

The plasma concentration time profile for bPiDDB suggests two-compartment model behavior with a rapid distribution phase, followed by a slower elimination phase. bPiDDB was well absorbed within 1 min. Comparison of the profiles for all three s.c. doses indicates that absorption of bPiDDB was rapid and independent of dose. The extremely rapid time to

reach peak plasma concentrations was unexpected, considering the high polarity and cationic nature of the molecule. Following s.c. dosing, concentrations of bPiDDB in plasma declined rapidly over 12–20 min, suggesting a significant distribution phase, consistent with bi-exponential disappearance from plasma. The terminal elimination half-life ($t_{1/2}$) was short (11–20 min), indicating the need for very short dosage intervals to maintain therapeutic levels. Elimination phases after s.c. and i.v. dosing were comparable, suggesting that absorption is even more rapid than elimination. Once absorbed, clearance of bPiDDB from the systemic circulation was large (3.3–5.0 mL/min) and did not change significantly with increasing dose (Table 1). After s.c. administration of bPiDDB, most of the drug is rapidly absorbed and undergoes little, if any, pre-systemic elimination before it reaches the systemic circulation. In addition, the clearance (0.6–0.9 L/h/kg) is large considering kidney and liver blood flow in rats (0.9 and 1.08 L/h/kg, respectively), suggesting that bPiDDB is efficiently removed by either the kidneys or the liver. Volume of distribution at steady state (V_{ss}; 10.2 L or 30 L/kg) also suggests that bPiDDB undergoes significant distribution into tissues. Thus, bPiDDB appears to distribute and bind to tissue proteins in the extracellular space and/or extracellular fluid. Since bPiDDB is a polar, cationic molecule, it is somewhat surprising to observe such marked tissue distribution. HPLC and radiometric analyses indicated the absence of metabolites in plasma supernatant 5–180 min after bPiDDB (5.6 mg/kg, s.c.; Figure 3). This lack of metabolism and the high F values results in direct systemic absorption of bPiDDB. Thus, the PK profile of bPiDDB (s.c.) shows rapid absorption and good bioavailability, affording adequate plasma concentrations for brain uptake possibly by facilitated transport.

In separate experiments, HPLC radiometric analysis of both brain homogenates and matched plasma samples from rats administered [$^{14}CH_3$]-bPiDDB (5.6 mg/kg, sc) showed only one [^{14}C]peak, identified as bPiDDB from co-elution with a UV-absorbing authentic standard (Table 2). As was observed in the above plasma PK studies, 100% recoveries of ^{14}C-radiolabel from the HPLC column were obtained in these brain homogenate and matched plasma samples (Table 2), again indicating the absence of measurable amounts of [^{14}C]-metabolites, both in plasma and in brain. Although bPiDDB was not detected in brain at 1 min post-injection, it was detected in plasma at this time point. Both plasma and brain bPiDDB concentrations peaked at 10 min and were in the range of 0.16–0.89 μg/ml and 0.09–0.33 μg/g, respectively. In contrast, the brain/plasma ratio increased over the first 10 min post injection, but did not significantly increase between 10 and 60 min post injection. Brain/plasma ratio values indicate that bPiDDB clearance from brain is slower than clearance from plasma. Although bPiDDB could be detected in plasma as early as 1 min post injection, a significant concentration of bPiDDB was only seen at 5 min post-drug treatment. The data clearly indicate that bPiDDB enters the brain from the vasculature, and may undergo sequestration in cells, extensive binding to brain tissues, or be simply trappe in brain tissue. Since bPiDDB is a polar molecule, it should be easily cleared from plasma by excretion via the kidney. This may explain the slower clearance of bPiDDB from the brain compared to plasma. These results support the contention that the polar, cationic bPiDDB molecule enters brain by facilitated transport, since it is unlikely that passive transport plays a role in the transport of bPiDDB into the CNS. These results are also consistent with our recent findings that bPiDDB accesses brain following systemic administration via the saturable BBB choline transporter (Lockman et al., 2006, 2008). We have also shown that after peripheral administration in rats, bPiDDB dose-dependently reduces nicotine-induced increases in extracellular DA by selectively blocking nAChRs involved in regulating DA release (Rahman et al., 2007), and that bPiDDB selectively and dose-dependently decreases nicotine reinforcement in rats at s.c. doses of 1, 3, and 5.6 mg/kg (Neugebauer et al., 2006; Bardo et al., unpublished results). A significant decrease in nicotine reinforcement was observed with bPiDDB at the 30 min time block in the rat behavioral study, when compared to saline; this compares favorably with a $t_{½}$ of ∼20 min for bPiDDB in the present study.

Since bPiDDB is not significantly metabolized in the rat, binding to plasma proteins and other tissue proteins may influence its PK profile. To determine the extent of binding of bPiDDB to plasma and brain supernatant protein, ultra-filtration studies were performed (Cheng et al., 2004). bPiDDB showed moderate plasma and brain supernatant protein binding (63–64% and 59–62%, respectively). In another series of experiments utilizing [$^{14}CH_3$]-bPiDDB, protein binding isotherms were generated for plasma and brain supernatant and bPiDDB binding was found to be fully reversible, as demonstrated by both plasma and brain supernatant isotherms intersecting at zero (Figure 5).

In summary, the results from this study show that the novel nAChR *bis*-quaternary ammonium antagonist bPiDDB is distributed rapidly from the s.c. site of injection into plasma, affords good plasma concentrations, and likely accesses brain tissues via facilitated transport by the blood-brain barrier choline transporter to afford therapeutically relevant brain concentrations.

Acknowledgments

This research was supported by National Institutes of Health Grant U19 DA017548.

Abbreviations

(PK)	Pharmacokinetic
bPiDDB	*N,N'*-dodecane-1,12-diyl-*bis*-3-picolinium dibromide
nAChRs	nicotinic acetyl choline receptors
BBB	blood-brain barrier
DA	dopamine
HPLC	high performance liquid chromatography
(LDA)	lithium diisopropylamide
$t_{1/2}$	half-life
C_{max}	maximum plasma concentration
T_{max}	time to reach maximum plasma concentration
AUC^{0-t}	area under the plasma concentration versus time curve from time zero to time t
$AUC^{0-\infty}$	area under the plasma concentration versus time curve from time zero to infinity
$AUC_{s.c.}$	area under the plasma concentration versus time curve from time zero to infinity after a subcutaneous dose
$AUC_{i.v.}$	area under the plasma concentration versus time curve from time zero to infinity after an intravenous dose
k	terminal elimination rate constant
V_{ss}	volume of distribution at steady state
CL	clearance
F	absolute bioavailability.

References

Allen DD, Lockman P, Roder KE, Dwoskin LP, Crooks PA. Active transport of high-affinity choline and nicotine analogs into the central nervous system by the blood-brain barrier choline transporter. J Pharmacol Exp Ther. 2003; 304:1268–1274. [PubMed: 12604705]

Ayers JT, Dwoskin LP, Deaciuc AG, Grinevich VP, Zhu J, Crooks PA. *bis*-Azaaromatic quaternary ammonium analogues: ligands for alpha$_4$beta$_2$* and alpha$_7$* subtypes of neuronal nicotinic receptors. Bioorg Med Chem Lett. 2002; 12:3067–3071. [PubMed: 12372503]

Chen JC, Mannino DM. Worldwide epidemiology of chronic obstructive pulmonary disease. Curr Opin Pulm Med. 1999; 2:93–99. [PubMed: 10813258]

Cheng Y, Ho E, Subramanyam B, Tseng J-L. Measurement of drug-protein binding by using immobilized human serum albumin liquid chromatography-mass spectrometry. J Chromatogr B. 2004; 809:67–73.

Coe JW, Brooks PR, Vetelino MG, Wirtz MC, Arnold EP, Huang J, Sands SB, Davis TI, Lebel LA, Fox CB, Shrikhande A, Heym JH, Schaeffer E, Rollema H, Lu Y, Mansbach RS, Chambers LK, Rovetti CC, Schulz DW, Tingley FD, O'Neill BT. Varenicline: An alpha4beta2 nicotinic receptor partial agonist for smoking cessation. J Med Chem. 2005; 48:3474–3477. [PubMed: 15887955]

Doggrell SA. Which is the best primary medication for long term smoking cessation-nicotine replacement therapy, bupropion or varenicline? Expert Opin Pharmacother. 2007; 8:2903–2915. [PubMed: 18001252]

Dwoskin LP, Crooks PA. Competitive neuronal nicotinic receptor antagonists: a new direction for drug discovery. Pharmacol Exp Ther. 2001; 298:395–402.

Dwoskin LP, Sumithran SP, Zhu J, Deaciuc AG, Ayers JT, Crooks PA. Subtype-selective nicotinic receptor antagonists: potential as tobacco use cessation agents. Bioorg Med Chem Lett. 2004; 14:1863–1867. [PubMed: 15050617]

Dwoskin LP, Rauhut AS, King-Pospisil KA, Bardo MT. Review of the pharmacology and clinical profile of bupropion, an antidepressant and tobacco use cessation agent. CNS Drug Rev. 2006; 12:178–207. [PubMed: 17227286]

Dwoskin LP, Matthew JB, Zheng G, Neugebauer NM, Manda VK, Lockman P, Papke R, Bardo MT, Crooks PA. Discovery of a novel nicotinic receptor antagonist for the treatment of nicotine addiction: 1-(3-picolinium)-12-triethylammonium-dodecane dibromide (TMPD). Biochem Pharmacol. 2007; 74:1271–1278. [PubMed: 17727820]

Geldenhuys WJ, Lockman PR, Nguyen TH, Van der Schyf CJ, Crooks PA, Dwoskin LP, Allen DD. 3D-QSAR study of *bis*-azaaromatic quaternary ammonium analogs at the blood-brain barrier choline transporter. Bioorg Med Chem. 2005; 13:4253–4261. [PubMed: 15878282]

Levine RR. The physiological disposition of hexamethonium and related compounds. J Pharmacol Exp Ther. 1960; 129:296–304. [PubMed: 14416282]

Lockman PR, Van der Schyf CJ, Abbruscato TJ, Allen DD. Chronic nicotine exposure alters blood-brain barrier permeability and diminishes brain uptake of methyllycaconitine. J Neurochem. 2005; 94:37–44. [PubMed: 15953347]

Lockman PR, Manda VK, Geldenhuys WJ, Mittapalli RK, Thomas F, Albayati ZF, Crooks PA, Dwoskin LP, Allen DD. Carrier-mediated transport of the quaternary ammonium neuronal nicotinic receptor antagonist, *N,N'*-dodecyl-*bis*-picolinium dibromide (bPiDDB) at the blood-brain barrier. J Pharmacol Exp Ther. 2008; 324:244–250. [PubMed: 17921191]

Lundahl LH, Henningfield JE, Lukas SE. Mecamylamine blockade of both positive and negative effects of IV nicotine in human volunteers. Pharmacol Biochem Behav. 2000; 66:637–643. [PubMed: 10899382]

Mannino DM, Braman S. The epidemiology and economics of chronic obstructive pulmonary disease. Proc Am Thorac Soc. 2007; 7:502–6. [PubMed: 17878461]

Maurer P, Bachmann MF. Vaccination against nicotine: an emerging therapy for tobacco dependence. Expert Opin Investig Drugs. 2007; 16:1775–1783.

Mihalak KB, Carroll FI, Leutje CW. Varenicline is a partial agonist at alpha4beta2 and full agonist at alpha7 neuronal nicotinic receptors. Mol Pharmacol. 2006; 70:801–805. [PubMed: 16766716]

Musick TJ, Gohdes M, Duffy A, Erickson DA, Krieter PA. Pharmacokinetics, disposition, and metabolism of bicifadine in the mouse, rat, and monkey. Drug Metab Dispos. 2007; 36:241–251. [PubMed: 17991767]

Neugebauer NM, Zhang Z, Crooks PA, Dwoskin LP, Bardo MT. Effect of a novel nicotinic receptor antagonist, *N*,*N*′-dodecane-1,12-diyl-bis-3-picolinium dibromide, on nicotine self-administration and hyperactivity in rats. Psychopharmacology. 2006; 189:426–434. [PubMed: 16220336]

Rahman S, Neugebauer NM, Zhang Z, Crooks PA, Dwoskin LP, Bardo MT. The effects of a novel nicotinic receptor antagonist *N*,*N*-dodecane-1,12-diyl-*bis*-3-picolinium dibromide (bPiDDB) on acute and repeated nicotine-induced increases in extracellular dopamine in rat nucleus accumbens. Neuropharmacology. 2007; 52:755–763. [PubMed: 17097117]

Teng L, Crooks PA, Buxton ST, Dwoskin LP. Nicotinic-receptor mediation of *S*(-)nornicotine-evoked [^{3}H]-overflow from rat striatal slices preloaded with [^{3}H]-dopamine. J Pharmacol Exp Ther. 1997; 283:778–787. [PubMed: 9353398]

Whittaker, ET.; Robinson, G. The Trapezoidal and Parabolic Rules. The Calculus of Observations: A Treatise on Numerical Mathematics. 4th ed.. New York: Dover; 1967. p. 156-158.

Zheng G, Sumithran SP, Deaciuc AG, Dwoskin LP, Crooks PA. *tris*-Azaaromatic quaternary ammonium salts: novel templates as antagonists at nicotinic receptors mediating nicotine-evoked dopamine release. Bioorg Med Chem Lett. 2007; 17:6701–6706. [PubMed: 17977723]

FIG. 1.
Chemical structure of *N*,*N*'-dodecane-1,12-diyl-*bis*-3-picolinium dibromide (bPiDDB). The asterisk indicates the location of the [^{14}C] radiolabel.

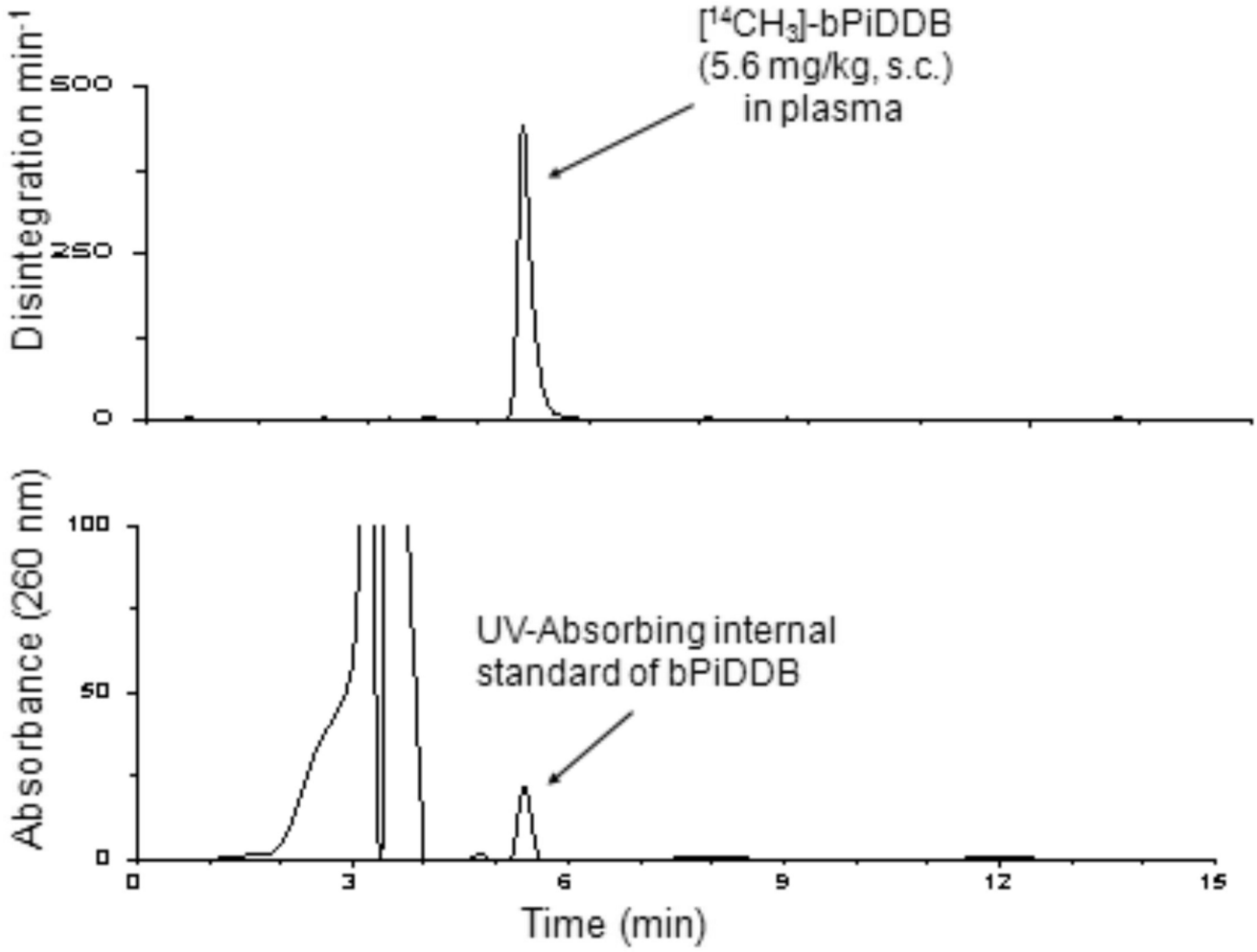

FIG. 2.

High pressure liquid radiochromatogram of plasma from a rat that had been dosed s.c. with [$^{14}CH_3$]-bPiDDB. An authentic UV-absorbing standard of bPiDDB was co-injected with the plasma sample. Top chromatogram: radioactivity in column effluents from a plasma sample of a rat that had been dosed s.c. with [$^{14}CH_3$]-bPiDDB determined by β-scintillation spectrometry. Bottom chromatogram: UV detection of co-injected standard at 260 nm. Chromatographic conditions for A and B were as described in the text.

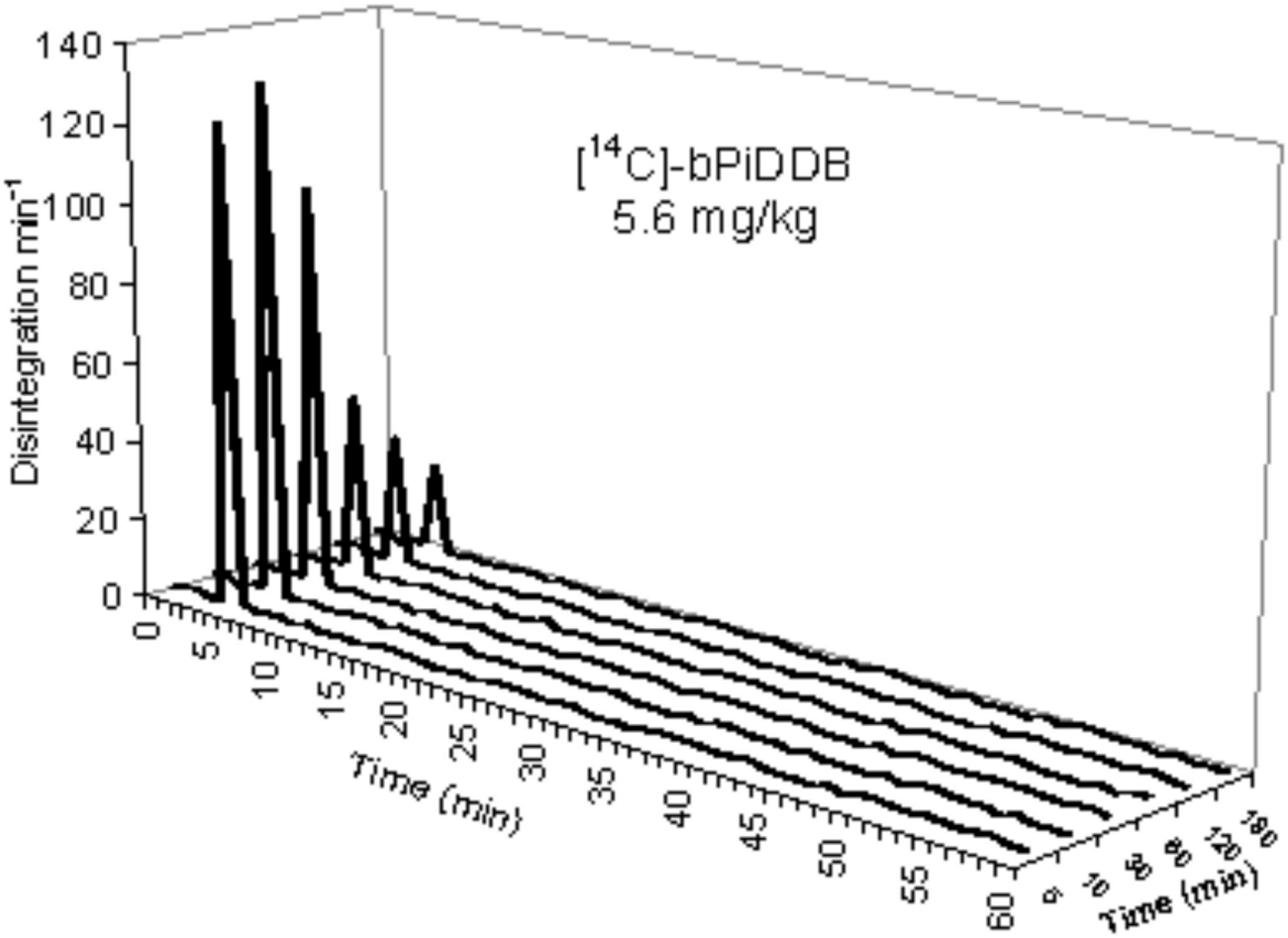

FIG. 3.

HPLC chromatogram of plasma radioactivity at 5, 10, 30 and 60 min following a single s.c. dose of 5.6 mg/kg [$^{14}CH_3$]-bPiDDB.

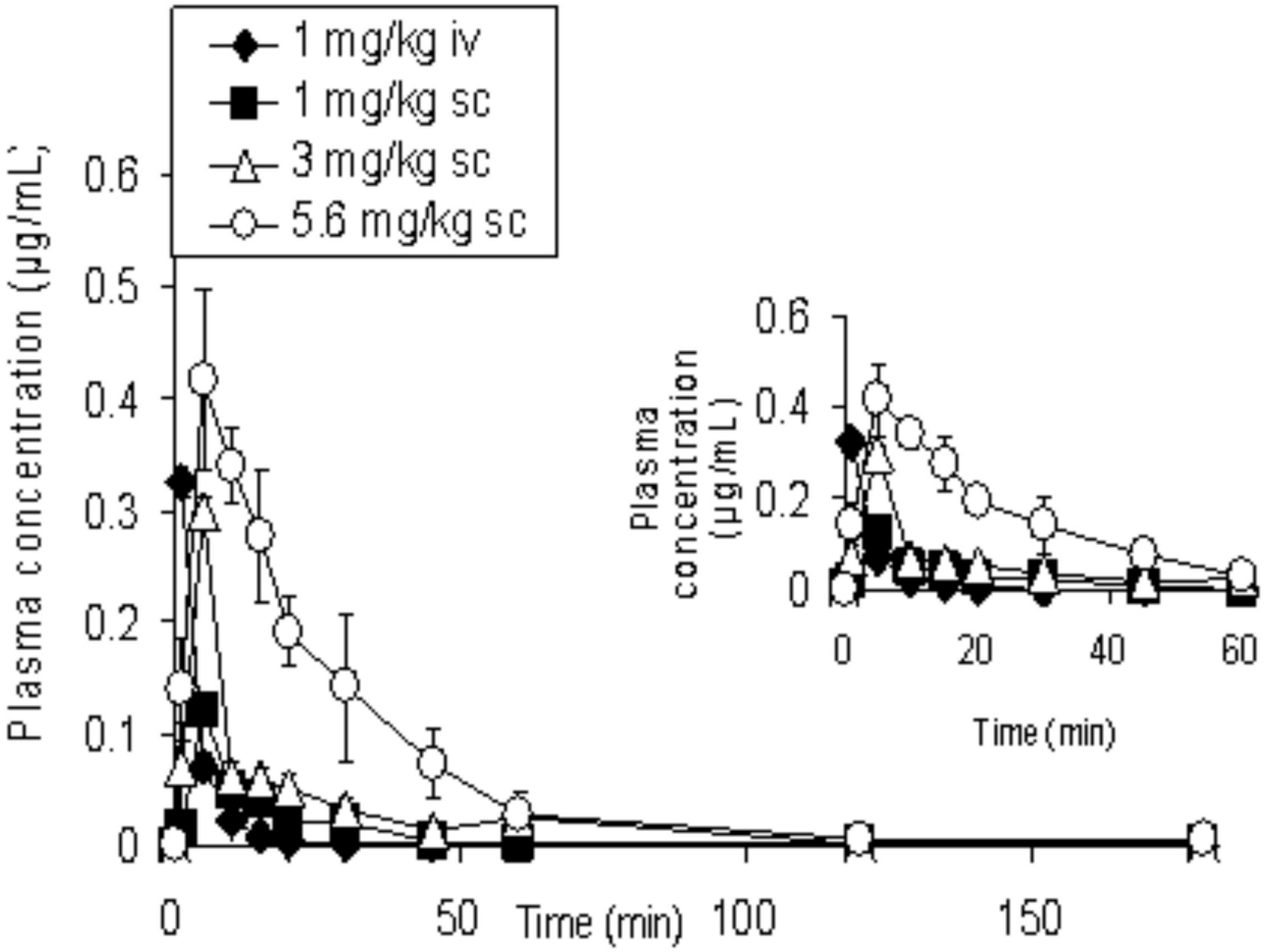

FIG. 4.

Plasma concentration-time ($AUC^{0–180}$) curves of bPiDDB in rats after intravenous (1 mg/kg) and subcutaneous administration (1, 3, 5.6 mg/kg) of [$^{14}CH_3$]-bPiDDB (n = 4–5). The curves in the inset represents $AUC^{0–60}$ of bPiDDB in rats after intravenous (1 mg/kg) and subcutaneous administration (1, 3, 5.6 mg/kg) of bPiDDB (n = 4–5). The analysis was carried out by β- scintillation spectrometry. All values show the mean ± SEM.

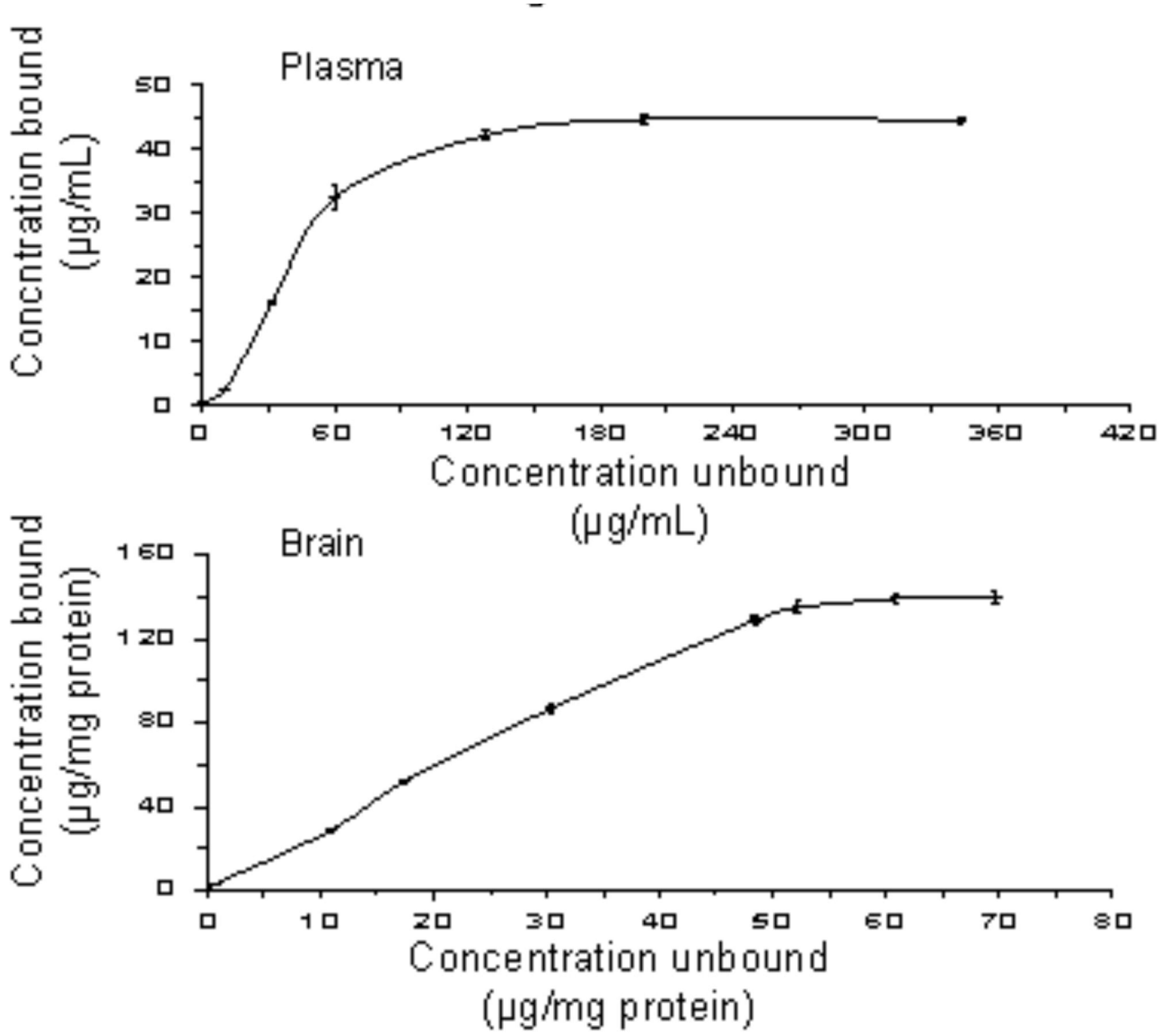

FIG. 5.

Top: hyperbolic plot of 1:1 protein binding isotherm of [$^{14}CH_3$]-bPiDDB in rat plasma. Results are mean ± SEM, n = 3. Bottom: hyperbolic plot of 1:1 protein binding isotherm of [$^{14}CH_3$]-bPiDDB in rat brain supernatant. Results are mean ± SEM, n = 3.

TABLE 1

Pharmacokinetic parameters of bPiDDB

Mean (± SEM) values for the pharmacokinetic parameters of bPiDDB following s.c. and i.v. administration.

Dose (route)	**1 mg/kg (s.c.)**	**3 mg/kg (s.c.)**	**5.6 mg/kg (s.c.)**	**1 mg/kg (i.v.)**
Parameter (units)				
$T_{max\ (min)}$	5.0 ± 0.00	6.7 ± 0.9	8.8 ± 2.3	–
C_{max} (μg/mL)	0.13 ± 0.01	0.33 ± 0.02*	0.43 ± 0.04*	0.33 ± 0.01
$t_{1/2}$ (min)	11.2 ± 1.6	19.5 ± 8.3	16.9 ± 1.3	11.9 ± 0.31
$AUC^{0-\infty}$ (μg.min/mL)	1.59 ± 0.3	4.1 ± 0.9*	11.5 ± 0.6*	1.98 ± 0.04
CL (L/h/kg)	0.6 ± 0.1	0.9 ± 0.1	0.7 ± 0.3	0.6 ± 0.03
F (%)	80.3	68.2	103.7	100
V_{ss} (L/kg)	–	–	–	30 ± 0.7

Values are mean ± SEM; n = 3–5.

* $p < 0.05$.

TABLE 2

Concentrations of bPiDDB in brain and plasma from bPiDDB-treated rats

Concentrations of bPiDDB in brain and plasma and brain/plasma ratios and percent recoveries of plasma and brain ^{14}C in rat plasma and brain at time points of 1, 5, 10, 15, 20 and 60 min, following administration of 5.6 mg/kg, s.c.

Time (min)	Plasma Conc. (μg/mL), n=4	Brain Conc. (μg/g), n = 4	Brain/Plasma ratio	% Recovery of Plasma $^{14}C^{*}$	% Recovery of Brain $^{14}C^{*}$
1	0.16 ± 0.03	0.01 ± 0.01#	0.06 ± 0.05	101 ± 0.5	99.8 ± 0.23
5	0.51 ± 0.01	0.09 ± 0.01	0.18 ± 0.01	98.4 ± 0.09	98.6 ± 0.03
10	0.89 ± 0.10	0.33 ± 0.06	0.37 ± 0.04	99.3 ± 0.11	99.7 ± 0.04
15	0.56 ± 0.09	0.21 ± 0.04	0.38 ± 0.11	98.7 ± 0.12	101 ± 0.03
20	0.41 ± 0.05	0.18 ± 0.03	0.46 ± 0.09	99.1 ± 0.06	102 ± 0.02
60	0.18 ± 0.02	0.10 ± 0.01	0.51 ± 0.15	98.2 ± 0.10	98.1 ± 0.02

* Indicates recovery of ^{14}C-radiolabel in the HPLC effluent.

Not significant compared to control